

NJC

Accepted Manuscript



This is an *Accepted Manuscript*, which has been through the Royal Society of Chemistry peer review process and has been accepted for publication.

Accepted Manuscripts are published online shortly after acceptance, before technical editing, formatting and proof reading. Using this free service, authors can make their results available to the community, in citable form, before we publish the edited article. We will replace this *Accepted Manuscript* with the edited and formatted *Advance Article* as soon as it is available.

You can find more information about *Accepted Manuscripts* in the [Information for Authors](#).

Please note that technical editing may introduce minor changes to the text and/or graphics, which may alter content. The journal's standard [Terms & Conditions](#) and the [Ethical guidelines](#) still apply. In no event shall the Royal Society of Chemistry be held responsible for any errors or omissions in this *Accepted Manuscript* or any consequences arising from the use of any information it contains.



www.rsc.org/njc

The effect of different alkyl chains on the photovoltaic performance of D- π -A porphyrin-sensitized solar cells

Jiangzhao Chen, Songguk Ko, Linfeng Liu, Yusong Sheng, Hongwei Han, Xiong Li*

Michael Grätzel Center for Mesoscopic Solar Cells, Wuhan National Laboratory for Optoelectronics, Huazhong University of Science and Technology, Wuhan 430074, Hubei, P. R. China

Abstract

In this study, a series of novel D- π -A porphyrin sensitizers with different alkyl chains were designed and synthesized for dye-sensitized solar cells. The effects of different alkyl chains (methyl, methoxyl and hexyloxy groups) on the photophysical, electrochemical and photovoltaic performance were investigated systematically. The results indicate that the molar extinction coefficients of three dyes normally increase as the alkyl chain length increases. Furthermore, it is also found that the incident photo-to-current conversion efficiencies(IPCEs), short circuit current(J_{sc}) and open circuit voltage(V_{oc}) of the dye-sensitized solar cells(DSSCs) based on **WH-C1**, **YD20** and **WH-C2** increase with the elongation of alkyl chains in the order of **WH-C1** < **YD20** < **WH-C2**. Accordingly, under standard global air mass 1.5 solar conditions, the optimized **WH-C2**-sensitized cell could produce a high conversion efficiency (η) of 7.77%, with a J_{sc} of 13.10 mA cm⁻², a V_{oc} of 831.10 mV, and a fill factor (FF) of 0.70.

* Correspondence author: Tel: +86 27 87793027; fax: +86 27 87793027

Email address: lxwhu2008@hotmail.com

Keywords: D- π -A porphyrin; Porphyrin dyes, dye-sensitized solar cells, structure-property relationship, different alkyl chains, recombination and aggregation, photovoltaic performance

1. Introduction

Dye-sensitized solar cells (DSSCs) as a promising photovoltaic device have attracted significant and extensive attention owing to their high power conversion efficiency, ease of fabrication and potential low cost compared with traditional silicon-based solar cells.¹⁻⁵ It is well known that DSSCs are principally composed of working electrodes(dye-sensitized nanocrystalline oxide), electrolytes or hole-transporting materials(HTMs), and counter electrodes (CEs), where the dyes play a crucial role in determining the power conversion efficiency(PCEs) of the devices. In the past two decades, Ru polypyridyl sensitizers with PCEs of over 11%⁶⁻⁹ have been demonstrated to be very efficient due to their broad absorption spectrum through metal-to-ligand charge transfer (MLCT), the longer exciton lifetime, and their long-term chemical stability.^{2, 5, 10} However, the high cost of noble metal ruthenium, the requirement for careful synthesis, tricky purification steps and low molar extinction coefficient¹⁰⁻¹² restrict its large-scale application.

Recently, due to its low cost, high molar extinction coefficients and structural diversity, the porphyrin has been paid a great deal of attention to be utilized as one of the most popular sensitizers for DSSCs.¹³⁻¹⁹ As we all know, most of efficient organic dyes have been designed according to basic structures of Donor- π -conjugated

bridge-Acceptor (simplified as D- π -A) which are beneficial to intramolecular electron transport. Inspired by this, the PCEs of the device sensitized by porphyrin have also been improved dramatically since the D- π -A structure was introduced into backbone of itself.²⁰⁻²⁷ At the same time, some high-performance D- π -A porphyrin dyes were designed rationally and synthesized for DSSCs.²⁸⁻³⁰ To our excitement, a record efficiency of 12.3% was achieved through the cosensitization of an organic dye **Y123** with the porphyrin **YD2-o-C8** based on D- π -A structure.³¹ In 2012, via substituting dihexyl diphenylamine donor in YD2-o-C8 with dimethoxytriphenylamine donor, the optimized push-pull porphyrin **YD20** has been successfully synthesized and produced a PCE of 8.1% based on I⁻/I₃⁻ electrolyte.³² Recently, the DSSCs based on dye **SM315** obtained through inserting benzothiadiazole unit between porphyrin ring and benzoic acid acceptor achieved a world record liquid state efficiency of 13% with the utilization of Cobalt (II/III) redox electrolyte.³³

Clearly, the performance of the DSSCs is closely related to molecular structures of sensitizers. Actually, the performance of porphyrin sensitized solar cells is limited by its serious aggregation and recombination, which also happen to the organic dyes.^{5, 34} However, in the fields of organic dyes, some measurements have been taken to surmount their above problems. For instance, incorporation of the long alkoxy chain onto the backbone of organic dyes could efficiently inhibit the aggregation and recombination, resulting in great enhancement of both the J_{sc} and V_{oc} .³⁵ As a matter of fact, dye intermolecular aggregation on the TiO₂ can also be inhibited through

introducing long alkyl chains at conjugated spacers to enhance J_{sc} .^{31-33, 36, 37} Additionally, incorporating long alkyl chains at donors can effectively suppress charge recombination between the electrons injected into conduction band of TiO_2 and oxidized dyes or electrolyte, resulting in an improvement of J_{sc} and V_{oc} .^{31, 33, 35-42} Therefore, based on the successful examples reported above on the organic dye, introducing long alkoxy chains onto the skeletons of the porphyrin dyes which usually possess some short alkoxy groups should be effective in inhibiting the intermolecular aggregation and electron recombination. Simultaneously, to date, the effect of different length alkyl chains on photovoltaic performance of porphyrin-sensitized solar cells was few reported.

In this context, one of the most widely used porphyrin dyes, **YD20** with short methoxy group, was selected as the reference dye. In order to further improve the PCEs of solar cells based on **YD20** as well as gain more insight into the relationship between the structure of porphyrin dyes and the performance of DSSCs, we design and synthesize two novel porphyrin molecules (denoted as **WH-C1** and **WH-C2**) through substituting the methoxy group on the donor of **YD20** with methyl and hexyloxy group, respectively. Furthermore, through photophysical, electrochemical, I-V curve, IPCE curve and EIS characterization methods, the relationship between the electron-donating ability and length of alkyl chains substituents at donors and the photovoltaic performance of the porphyrin-sensitized solar cells was systematically investigated. As a result, the optimized device sensitized by **WH-C2** with long hexyloxy group shows a best PCE of 7.7%.

2. Experimental

2.1 Materials

All reagents and solvents were obtained from commercial sources and used without further purification unless otherwise noted. THF and toluene was dried over sodium/benzophenone and freshly distilled before use. DMF used for formylation was dried over enough P_2O_5 for several hours and distilled under reduced pressure. Column chromatography of all the products was performed on silica gel (Kanto, Silica Gel 60N, spherical, 200–300 mesh), and some were further purified by recrystallization.

2.2 Characterization

UV-visible spectra of about $4\mu\text{m}$ thick TiO_2 film sensitized by as-synthesized dyes were performed on PerKinElmer Lambda 950 spectrophotometer. ^1H NMR and ^{13}C NMR spectra were recorded on Bruker-AV400 spectrometers with 400 MHz. The chemical shifts were recorded in parts per million (ppm) with TMS as the internal reference. ESI mass spectra were measured on Finnigan LCQ Advantage mass spectrometer. The cyclic voltammeters (CVs) were carried out with a three-electrode system in an argon-purged electrolyte solution on PARSTAT 2273 Electrochemical Workstation. Cyclic voltammograms for porphyrin dyes were conducted with a three-electrode cell equipped with a BAS glassy carbon (0.07 cm^2) disk as the working electrode, a platinum wire as the auxiliary electrode, and a Ag/AgCl (saturated) reference electrode. The working electrode was polished with $0.03\ \mu\text{m}$ alumina on felt pads (Buehler) and treated ultrasonically for 1 min before each

experiment. The potential of the reference electrode was adjusted by recording the cyclic voltammogram for 0.01 M ferrocene in THF containing 0.1 M TBAPF₆. The thickness of the films was measured with a profilometer (VeecoDektak 150). The melting points of **WH-C2**, **YD20** and **WH-C1** were measured on a Melting point meter, SG WRR, Shanghai Shenguang.

2.3 Synthesis

N,N-bis(4-methylphenyl)-N-(4-iodophenyl) amine (1)

Compound **1** was prepared according to literature procedure.^{43, 44} To the solution of 4,4-dimethyltriphenylamine(1.093g, 4mmol) in 100mL HOAC were KI(0.332g, 2mmol) and KIO₃(0.428g, 2mmol) and was refluxed under dinitrogen for 14 h. The progress of the reaction was monitored with TLC. After finishing reacting, saturated NaHSO₃(aq) were added slowly into the reaction flask until the reaction solution turned from reddish brown to colourless. After extraction with DCM, The combined extracts were dried over anhydrous MgSO₄ and the solvent was removed under reduced pressure. The residue was purified by column chromatography (silica gel) using petroleum ether as eluent to give a white solid **1**(1.29g, 81%). ¹HNMR (CDCl₃, 600 MHz) δ_H 7.43 (d, *J* = 8.6 Hz, 2H), 7.06 (d, *J* = 8.2 Hz, 4H), 6.97 (d, *J* = 8.2Hz, 4H), 6.76 (d, *J* = 8.6 Hz, 2H), 2.30 (s, 2H). ¹³C NMR (CDCl₃, 600 MHz) δ_C 148.1, 144.8, 137.8, 133.1, 130.0, 124.8, 124.1, 83.5, 20.9. APCI-MS: m/z calcd for ([M+1]⁺) C₂₀H₁₈IN 400.2681, found 400.2680.

p-iodoanisoole (2)

Compound **2** was prepared under modified conditions of a literature procedure.³¹

A mixture of 4-iodophenol (26.4 g, 120 mmol), methyl iodide (17.03 g, 120 mmol) and K_2CO_3 (82.8 g, 600 mmol) in 400 mL of Acetone was stirred at 60 °C for 16 h. After cooling to room temperature, the mixture was poured into 100 mL water and extracted with ether. The combined organic phase was evaporated under vacuum to remove the solvent. The residue was subjected to silica gel column chromatography, eluting with a mixture of hexane to give a white crystal (25.56g, 91%). 1H NMR ($CDCl_3$, 400 MHz) δ_H 7.58 (d, $J = 8.9$ Hz, 2H), 6.71 (d, $J = 8.9$ Hz, 2H), 3.80 (s, 3H). ^{13}C NMR ($CDCl_3$, 400 MHz) δ_C 159.5, 138.2, 116.4, 82.7, 55.3. APCI-MS: m/z calcd for $([M]^+)$ C_7H_7IO 234.0343, found 234.0342.

4,4-Dimethoxytriphenylamine (3)

Compound **3** was prepared according to literature procedure.^{37, 45} To a stirred solution of aniline (1.962g, 21.07 mmol), **2** (12.328 mg, 52.675 mmol), CuI (0.802 g, 4.213 mmol) and 1,10-phenantroline (0.758 g, 4.213 mmol) in 150 mL toluene was added t-BuOK (18.91 g, 168.56 mmol) under N_2 , the mixture was heated to 120 °C, and reacted for 9 h. After cooling to room temperature, the mixture was extracted with CH_2Cl_2 and the organic layer was washed with water. The organic layer was combined and dried over anhydrous magnesium sulfate. After removing solvent under reduced pressure, the residue was purified by column chromatography (ethyl acetate/petroleum ether 60–90 °C, 1/50, v/v) on silica gel to yield a white powder (4.31g, 67%). 1H NMR ($CDCl_3$, 600 MHz) δ_H 7.17 (t, $J = 7.9$ Hz, 2H), 7.04 (d, $J = 8.9$ Hz, 4H), 6.93 (d, $J = 7.7$ Hz, 2H), 6.86 (t, $J = 7.3$ Hz, 1H), 6.82 (d, $J = 8.9$ Hz, 4H), 3.79 (s, 6H). ^{13}C NMR ($CDCl_3$, 600 MHz) δ_C 155.7, 148.8, 141.1, 128.9, 126.4,

120.9, 120.6, 114.6, 55.5. APCI-MS: m/z calcd for $([M]^+)$ $C_{20}H_{19}NO_2$ 305.3704, found 305.3702.

N,N-bis(4-methoxyphenyl)-N-(4-iodophenyl) amine (4)

Compound **4** was synthesized from 4,4-dimethoxytriphenylamine (1.221g,4mmol) according to the procedure as described above for synthesis of **1**, giving a yellow solid (1.294g,75%). 1H NMR ($CDCl_3$, 600 MHz) δ_H 7.23 (d, $J = 8.9$ Hz, 2H), 7.02 (d, $J = 8.8$ Hz, 4H), 6.82 (d, $J = 8.9$ Hz, 4H), 6.79 (d, $J = 8.8$ Hz, 2H), 3.79 (s, 6H). ^{13}C NMR ($CDCl_3$, 600 MHz) δ_C 156.0, 150.0, 140.5, 131.8, 126.6, 121.9, 114.8, 112.3, 55.5. APCI-MS: m/z calcd for $([M+1]^+)$ $C_{20}H_{18}INO_2$ 432.2669, found 432.2668.

4-iodophenyl hexyl ether (5)

Compound **5** was prepared according to literature procedure.³¹ A mixture of 4-iodophenol (26.4 g, 120 mmol), 1-bromohexane (17.03 g, 120 mmol) and K_2CO_3 (82.8 g, 600 mmol) in 400 mL of Acetone was stirred at 60 °C for 16 h. The solvent was removed under reduced pressure and extracted with EtOAc (3×100 mL). The combined extracts were washed with water and dried over anhydrous $MgSO_4$. After removal of solvent under reduced pressure, the product was purified by column chromatography eluting with hexanes to give a colorless oil (26.5g, 79%). 1H NMR ($CDCl_3$, 400 MHz) δ_H 7.52 (d, $J = 9.0$ Hz, 2H), 6.66 (d, $J = 9.0$ Hz, 2H), 3.89 (t, $J = 6.6$ Hz, 2H), 1.78 – 1.71 (m, 2H), 1.47 -1.40 (m, 2H), 1.36 – 1.30 (m, 4H), 0.90 (t, $J = 7.0$ Hz, 3H). ^{13}C NMR ($CDCl_3$, 400 MHz) δ_C 159.1, 138.2, 117.0, 82.4, 68.2, 31.6, 29.1, 25.7, 22.6, 14.0. APCI-MS: m/z calcd for $([M]^+)$ $C_{12}H_{17}IO$ 304.1672, found

304.1672.

4,4-Dihexyloxytriphenylamine (6)

Compound **6** was synthesized from 4-iodophenyl hexyl ether (16.023g, 52.675 mmol) according to the procedure as described above for synthesis of **3**, giving a yellow oil (6.67g, 71%). ^1H NMR (CDCl_3 , 600 MHz) δ_{H} 7.13 (t, $J = 7.8$ Hz, 2H), 7.00 (d, $J = 8.8$ Hz, 4H), 6.92 (d, $J = 8.0$ Hz, 2H), 6.82 (t, $J = 7.3$ Hz, 1H), 6.79 (d, $J = 8.9$ Hz, 4H), 3.90 (t, $J = 6.5$ Hz, 4H), 1.78 – 1.73 (m, 2H), 1.47 – 1.44 (m, 4H), 1.34 – 1.33 (m, 8H), 0.90 (t, $J = 6.7$ Hz, 6H). ^{13}C NMR (CDCl_3 , 600 MHz) δ_{C} 155.4, 148.9, 141.1, 128.9, 126.5, 120.9, 117.0, 115.3, 68.3, 31.7, 29.4, 25.8, 22.7, 14.1. APCI-MS: m/z calcd for ($[\text{M}]^+$) $\text{C}_{30}\text{H}_{39}\text{NO}_2$ 445.6362, found 445.6361.

N,N-bis(4-hexyloxyphenyl)-N-(4-iodophenyl) amine (7)

Compound **7** was synthesized from 4,4-dihexyloxytriphenylamine (1.783g, 4mmol) according to the procedure as described above for synthesis of **1**, giving a yellow oil (1.806g, 79%). ^1H NMR (CDCl_3 , 600 MHz) δ_{H} 7.23 (d, $J = 8.9$ Hz, 2H), 7.02 (d, $J = 8.8$ Hz, 4H), 6.82 (d, $J = 8.9$ Hz, 4H), 6.79 (d, $J = 8.8$ Hz, 2H), 4.11 (t, $J = 6.4$ Hz, 4H), 2.02 – 1.95 (m, 4H), 1.72 – 1.65 (m, 4H), 1.59 – 1.55 (m, 8H), 1.15 (t, $J = 6.7$ Hz, 6H). ^{13}C NMR (CDCl_3 , 600 MHz) δ_{C} 155.9, 148.2, 140.6, 129.1, 126.7, 122.0, 115.6, 112.4, 68.4, 31.8, 29.5, 26.0, 22.8, 14.2. APCI-MS: m/z calcd for ($[\text{M}]^+$) $\text{C}_{30}\text{H}_{38}\text{INO}_2$ 571.5327, found 571.5324.

dipyrromethane (8)

Compound **8** was prepared by adapting the literature procedure.^{46, 47} Formaldehyde (3g, 90mmol) was added to pyrrole (150 mL, 2.16 mol) and the

solution degassed by stirring under reduced pressure and flushing with N₂. TFA (0.81 mL, 10.9 mmol) was added with vigorous stirring, and the reaction was allowed to proceed for 15 min at room temperature before NaOH (0.2M×100 mL). The product was extracted by DCM and washed with water (3×100 mL). The combined extracts were dried over anhydrous MgSO₄. After removal of DCM under diminished pressure, excess pyrrole was distilled out under reduced pressure. And then the crude product was purified by column chromatography eluted with ethyl acetate and petroleum ether mixture, giving the product as a colourless crystalline solid (6.97g, 53%). ¹H NMR (CDCl₃, 400 MHz) δ_H 7.54 (br. s, 2H), 6.54 (m, 2H), 6.13 (m, 2H), 6.01 (m, 2H), 3.87 (s, 2H). ¹³C NMR (CDCl₃, 400 MHz) δ_C 129.2, 117.5, 108.3, 106.6, 26.4. APCI-MS: m/z calcd for ([M]⁺) C₉H₁₀N₂ 146.1891, found 146.1892.

1,3-Dioctoxybenzene (9)

Compound **9** was prepared according to literature procedure.³¹ A mixture of resorcinol (11 g, 0.1 mol), 1-bromooctane (69.6mL,0.4mol) and K₂CO₃(69g,0.5mol) was refluxed for 4 days in dry acetone (500mL).The solvent was removed under reduced pressure and extracted with EtOAc (3×100mL). The combined extracts were washed with water and dried over anhydrous MgSO₄. After removal of solvent under reduced pressure, the product was purified by column chromatography eluting with hexanes to give 1,3-di(octyloxy)benzene (26.5g,79%). ¹H NMR (CDCl₃, 400 MHz) δ_H 7.13 (t, *J* = 8.4 Hz, 1H), 6.46 (m, 3H), 3.92 (t, *J* = 6.6 Hz, 4H), 1.79-1.72 (m, 4H), 1.47-1.40 (m, 4H), 1.35-1.23 (m, 16H), 0.88 (t, *J* = 6.7 Hz, 6H). ¹³C NMR (CDCl₃, 400 MHz) δ_C 160.4, 129.7, 106.7, 101.5, 68.0, 31.8, 29.4, 29.3, 29.2, 26.1, 22.7, 14.1.

APCI-MS: m/z calcd for $([M+1]^+)$ $C_{22}H_{38}O_2$ 335.5359, found 335.5368.

2,6-Dioctoxybenzaldehyde (10)

Compound **10** was prepared according to literature procedure.³¹ A three-neck flask was equipped with an additional funnel and charged with compound **9** (10 g, 0.03 mol) and tetramethylethylenediamine (TMEDA) (1.15 mL) in 84 mL of tetrahydrofuran. The solution was degassed with dinitrogen for 15 min and cooled to 0°C, and then *n*-butyllithium (22.4 mL, 1.6 M solution in hexanes 0.036 mol) was added dropwise over 20 min and allowed to stir for 3 h. After warming to room temperature, dimethylformamide (DMF) (4.38 mL, 0.06 mol) was added dropwise, and the reaction was stirred for an additional 2 h. The reaction was quenched with water, and the mixture was extracted with ether (3×80 mL), dried over anhydrous $MgSO_4$, and the solvent was removed under reduced pressure. The product was recrystallized from hexanes to yield a white solid (8.67 g, 80% yield). 1H NMR ($CDCl_3$, 400 MHz) δ H 10.54 (s, 1H), 7.37 (t, $J = 8.4$ Hz, 1H), 6.52 (d, $J = 8.5$ Hz 2H), 4.01 (t, $J = 6.5$ Hz, 4H), 1.85-1.78 (m, 4H), 1.50-1.43 (m, 4H), 1.36-1.28 (m, 16H), 0.88 (t, $J = 6.9$ Hz, 6H). ^{13}C NMR ($CDCl_3$, 400 MHz) δ C 189.2, 161.7, 135.5, 114.8, 104.5, 68.9, 31.8, 29.3, 29.2, 29.1, 26.0, 22.6, 14.1. APCI-MS: m/z calcd for $([M+1]^+)$ $C_{23}H_{38}O_3$ 363.5460, found 363.5457.

5,15-Bis(2,6-dioctoxyphenyl)porphyrin (11)

Compound **11** was synthesized according to literature procedure.³¹ To a degassed solution of dipyrromethane (6.04 g, 41.4 mmol) and compound **10** (15 g, 41.4 mmol) in DCM (5.4 L) was added trifluoroacetic acid (2.75 mL, 37.3 mmol). After the

solution was stirred at 23 °C under dinitrogen for 4 h, DDQ (14.1 g, 62.1 mmol) was added and the mixture was stirred for an additional 1 h. The mixture was basified with Et₃N (7 mL) and filtered through silica. The solvent was removed under reduced pressure and the residue was purified by column chromatography (silica gel) using DCM/hexanes = 1/2 as eluent. The product was recrystallized from MeOH/CH₂Cl₂ to give the product (6.07 g, 30.1%) as a purple powder. ¹H NMR (CDCl₃, 400 MHz) δ_H 10.12 (s, 2H), 9.24 (d, *J* = 4.6 Hz, 4H), 8.96 (d, *J* = 4.5 Hz, 4H), 7.68 (t, *J* = 8.4 Hz, 2H), 7.00 (d, *J* = 8.5 Hz, 4H), 3.82 (t, *J* = 6.4 Hz, 8H), 0.95-0.87 (m, 8H), 0.85-0.78 (m, 8H), 0.66-0.59 (m, 8H), 0.56-0.50 (m, 28H), 0.48-0.40 (m, 8H), -2.99 (s, 2H). ¹³C NMR (CDCl₃, 400 MHz) δ_C 160.2, 147.7, 145.0, 130.8, 130.4, 130.0, 120.1, 111.6, 105.4, 103.9, 68.8, 31.3, 28.6, 25.3, 22.3, 13.8. APCI-MS: *m/z* calcd for ([M+1]⁺) C₆₄H₈₆N₄O₄ 976.3920, found 976.3921.

5,15-Dibromo-10,20-bis(2,6-dioctoxyphenyl)porphyrin (12)

Compound **12** was synthesized according to literature procedure.^{23, 32} Compound **11** (4.836g, 4.96mmol) was dissolved in chloroform (300mL) with pyridine (2.6mL). A solution of NBS (1.768g, 9.92mmol) in chloroform (100mL) and pyridine (1.4mL) was added dropwise at 0°C over 30min. The reaction was stirred for 15min and then quenched with acetone (10mL). The solvents were removed under reduced pressure and the residue was purified by column chromatography (silica gel) using DCM/hexanes = 1/4 (volume ratio) as eluent. The product was recrystallized from THF/MeOH to give the product (5.18g, 92.2%) as a purple powder. ¹H NMR (CDCl₃, 400 MHz) δ_H 9.50 (d, *J* = 4.8 Hz, 4H), 8.78 (d, *J* = 4.6 Hz, 4H), 7.69 (t, *J* = 8.4 Hz,

2H), 6.97 (d, $J = 8.4$ Hz, 4H), 3.83 (t, $J = 6.4$ Hz, 8H), 0.98–0.91 (m, 8H), 0.84–0.76 (m, 8H), 0.69–0.56 (m, 8H), 0.53–0.48 (m, 28H), 0.46–0.37 (m, 8H), -2.59 (s, 2H). ^{13}C NMR (CDCl_3 , 400 MHz) δ_{C} 160.0, 151.5, 149.8, 132.9, 130.1, 120.8, 115.0, 105.2, 104.0, 68.6, 31.3, 28.6, 25.3, 22.2, 13.8. APCI-MS: m/z calcd for $([\text{M}]^+)$ $\text{C}_{64}\text{H}_{84}\text{Br}_2\text{N}_4\text{O}_4$ 1133.1841, found 1133.1834.

[5,15-Dibromo-10,20-bis(2,6-di-octoxyphenyl)porphinato] zinc(II) (13)

Compound **13** was prepared under modified conditions of literature procedure.³¹ A suspension of **12** (4g, 3.52 mmol) and $\text{Zn}(\text{OAc})_2 \cdot 2\text{H}_2\text{O}$ (6.476g, 35.2 mmol) in a mixture of DCM (400 mL) and MeOH (200 mL) was stirred at RT overnight. The reaction was quenched with water (100 mL), and the mixture was extracted with DCM (2×100 mL). The combined extracts were washed with water and dried over anhydrous MgSO_4 . The solvent was removed under reduce pressure to give the product (3.92g, 93.1%). ^1H NMR (CDCl_3 , 400 MHz) δ_{H} 9.62 (d, $J = 4.6$ Hz, 4H), 8.88 (d, $J = 4.6$ Hz, 4H), 7.69 (t, $J = 8.4$ Hz, 2H), 6.99 (d, $J = 8.4$ Hz, 4H), 3.83 (t, $J = 6.4$ Hz, 8H), 0.97–0.91 (m, 8H), 0.86–0.74 (m, 8H), 0.61–0.54 (m, 8H), 0.53–0.41 (m, 28H), 0.39–0.32 (m, 8H). ^{13}C NMR (CDCl_3 , 400 MHz) δ_{C} 159.9, 151.4, 149.7, 132.8, 130.0, 120.7, 114.9, 105.2, 103.9, 68.6, 31.3, 28.6, 25.2, 22.2, 13.8. APCI-MS: m/z calcd for $([\text{M}+1]^+)$ $\text{C}_{64}\text{H}_{82}\text{Br}_2\text{N}_4\text{O}_4\text{Zn}$ 1197.5773, found 1197.5715.

[5,15-Bis(2,6-di-octoxyphenyl)-10,20-Bis[(triisopropylsilyl)ethynyl]-porphinato] zinc(II) (14)

Compound **14** was prepared according to literature procedure.³¹ A mixture of the zinc complex of **13** (0.910g, 0.81 mmol), (triisopropylsilyl)acetylene (0.906 mL,

4.08mmol), Pd(PPh₃)₂Cl₂ (0.220g, 0.32 mmol), CuI (0.094g, 0.48mmol), THF (60 mL) and NEt₃ (10mL) was refluxed at 65 °C for 4 h under dinitrogen. The solvent was removed under vacuum. The residue was purified by column chromatography(silica gel) using DCM/hexanes = 1/20 to as eluent to give the product (0.97 g, 85.7%) as a purple solid. ¹H NMR (CDCl₃, 400 MHz) δ_H 9.66 (d, *J* = 4.6 Hz, 4H), 8.86 (d, *J* = 4.6 Hz, 4H), 7.66 (t, *J* = 8.4 Hz, 2H), 6.98 (d, *J* = 8.4 Hz, 4H), 3.81 (t, *J* = 6.4 Hz, 8H), 1.48–1.41 (m, 42H), 0.99–0.86 (m, 8H), 0.79–0.70 (m, 8H), 0.58–0.51 (m, 8H), 0.51–0.45 (m, 28H), 0.44–0.33 (m, 8H). ¹³C NMR (CDCl₃, 400 MHz) δ_C 159.9, 152.0, 150.7, 131.7, 130.9, 130.8, 121.0, 114.9, 110.1, 105.4, 100.2, 96.5, 68.8, 31.2, 28.5, 25.2, 22.1, 19.1, 13.7, 11.9. APCI-MS: *m/z* calcd for ([M+1]⁺) C₈₆H₁₂₄N₄O₄Si₂Zn 1400.2541, found 1400.2518.

5-(4-carboxy-phenyl)ethynyl-15-(4-(N,N-bis(4-methylphenyl)amino)-phenylethynyl)-10,20-bis(2,6-di-octoxyphenyl phenyl)porphinato zinc(II) (WH-C1)

Compound **WH-C1** was prepared according to literature procedure.^{21, 23, 32} To a solution of porphyrin **14** (98 mg, 0.07 mmol) in dry THF (20 mL) was added TBAF (1M in THF, 0.57 mL, 0.57 mmol). The solution was stirred at room temperature for 0.5 h. The mixture was concentrated and then extracted with CH₂Cl₂/H₂O. The organic layer was dried over anhydrous MgSO₄ and the solvent was removed under vacuum. The residue, N,N-bis(4-methylphenyl)-N-(4-iodophenyl) amine (31 mg, 0.077 mmol, 1.0eq), and 4-iodobenzoic acid (17 mg, 0.07mmol, 1.0eq) were dissolved in a mixture of THF (20 mL) and Et₃N (4 mL) and degassed with N₂ for 10 min, and then Pd₂(dba)₃ (33 mg, 0.036 mmol) and AsPh₃ (88 mg, 0.29mmol) were

added to the mixture. The solution was refluxed for 5 h under N₂ and the solvent was removed under reduced pressure. The residue was purified on a column chromatography (silica gel) using CH₂Cl₂/CH₃OH = 20/1 as eluent. Recrystallization from CH₂Cl₂/EtOH gave a green solid (40 mg, 38.7%). ¹H NMR (CDCl₃/pyridine-d₅, 600 MHz) δ_H 9.62 (dd, *J* = 7.5, 4.5 Hz, 4H), 8.88 (d, *J* = 4.3 Hz, 2H), 8.84 (d, *J* = 4.3 Hz, 2H), 8.32 (d, *J* = 8.1 Hz, 2H), 8.02 (d, *J* = 8.0 Hz, 2H), 7.77 (d, *J* = 8.5 Hz, 2H), 7.72 (t, *J* = 8.5 Hz, 2H), 7.14 (d, *J* = 8.6 Hz, 4H), 7.11 (d, *J* = 8.4 Hz, 2H), 7.09 (d, *J* = 8.2 Hz, 4H), 7.04 (d, *J* = 8.6 Hz, 4H), 3.86 (t, *J* = 6.2 Hz, 8H), 2.33 (s, 6H), 1.32–1.23 (m, 8H), 0.95–0.90 (m, 8H), 0.75–0.68 (m, 8H), 0.61–0.54 (m, 28H), 0.48–0.41 (m, 8H). ¹³C NMR (CDCl₃/pyridine-d₅, 600 MHz) δ_C 159.8, 151.5, 151.2, 150.5, 150.4, 148.0, 144.7, 132.2, 130.9, 129.9, 129.6, 125.0, 121.4, 121.2, 116.6, 114.9, 105.0, 100.8, 96.9, 94.5, 92.8, 68.4, 31.3, 28.6, 28.5, 25.2, 22.2, 20.7, 13.8. ESI-MS: *m/z* calcd for ([M]⁺) C₉₅H₁₀₅N₅O₆Zn: 1478.2891; found 1478.2886. mp: 249°C.

5-(4-carboxy-phenyl)ethynyl-15-(4-(N,N-bis(4-methoxyphenyl)amino)-phenylethynyl)-10,20-bis(2,6-di-octoxyphenyl phenyl)porphinato zinc(II) (YD20)

Compound **YD20** was synthesized from N,N-bis(4-methoxyphenyl)-N-(4-iodophenyl) amine (33 mg, 0.077 mmol, 1.0 eq) according to the procedure as described above for synthesis of **WH-C1**, giving a green solid (30 mg, 28.4%). ¹H NMR (CDCl₃/pyridine-d₅, 600 MHz) δ_H 9.62 (dd, *J* = 7.5, 4.5 Hz, 4H), 8.88 (d, *J* = 4.4 Hz, 2H), 8.84 (d, *J* = 4.2 Hz, 2H), 8.32 (d, *J* = 6.7 Hz, 2H), 8.01 (d, *J* = 6.2 Hz, 2H), 7.75 (d, *J* = 8.3 Hz, 2H), 7.72 (t, *J* = 8.5 Hz, 2H),

7.16 (d, $J = 6.8$ Hz, 4H), 7.04 (d, $J = 6.8$ Hz, 2H), 7.01 (d, $J = 6.4$ Hz, 4H), 6.89 (d, $J = 6.8$ Hz, 4H), 3.86 (t, $J = 5.9$ Hz, 8H), 3.78 (s, 6H), 1.38–1.21 (m, 8H), 1.01–0.84 (m, 8H), 0.80–0.69 (m, 8H), 0.66–0.51 (m, 28H), 0.50–0.40 (m, 8H). ^{13}C NMR ($\text{CDCl}_3/\text{pyridine-d}_5$, 600 MHz) δ_{C} 159.8, 156.2, 151.5, 151.2, 150.4, 150.3, 149.5, 140.2, 132.1, 131.6, 131.2, 130.8, 129.9, 121.1, 119.5, 115.4, 114.7, 105.0, 101.1, 96.9, 94.5, 92.5, 68.3, 55.3, 31.3, 29.5, 28.6, 28.5, 25.1, 22.2, 13.8. ESI-MS: m/z calcd for $([\text{M}]^+)$ $\text{C}_{95}\text{H}_{105}\text{N}_5\text{O}_8\text{Zn}$: 1510.2879; found 1510.2878. mp: 238°C.

5-(4-carboxy-phenyl)ethynyl-15-(4-(N,N-bis(hexyloxyphenyl)amino)-phenylethynyl)-10,20-bis(2,6-di-octoxyphenyl phenyl)porphinato zinc(II) (WH-C2)

Compound **WH-C2** was synthesized from N,N-bis(4-methoxyphenyl)-N-(4-iodophenyl) amine (33mg, 0.077mmol, 1.0eq) according to the procedure as described above for synthesis of **WH-C1**, giving a green solid (37mg, 32%). ^1H NMR ($\text{CDCl}_3/\text{pyridine-d}_5$, 600 MHz) δ_{H} 9.61 (dd, $J = 7.5, 4.5$ Hz, 4H), 8.88 (d, $J = 4.3$ Hz, 2H), 8.84 (d, $J = 4.3$ Hz, 2H), 8.32 (d, $J = 7.9$ Hz, 2H), 8.02 (d, $J = 7.9$ Hz, 2H), 7.76 (d, $J = 8.4$ Hz, 2H), 7.72 (t, $J = 8.5$ Hz, 2H), 7.15 (d, $J = 8.6$ Hz, 4H), 7.10 (d, $J = 8.3$ Hz, 2H), 7.03 (d, $J = 8.5$ Hz, 4H), 6.89 (d, $J = 8.7$ Hz, 4H), 3.95 (t, $J = 6.2$ Hz, 4H), 3.87 (t, $J = 5.7$ Hz, 8H), 3.82 (s, 6H), 1.80–1.75 (m, 4H), 1.50–1.42 (m, 4H), 1.38–1.31 (m, 8H), 1.29–1.23 (m, 8H), 0.97–0.85 (m, 14H), 0.76–0.68 (m, 8H), 0.62–0.52 (m, 28H), 0.48–0.40 (m, 8H). ^{13}C NMR ($\text{CDCl}_3/\text{pyridine-d}_5$, 600 MHz) δ_{C} 159.8, 155.8, 151.5, 151.2, 150.5, 150.3, 148.6, 140.0, 132.2, 130.8, 130.3, 129.8, 126.9, 121.2, 119.4, 115.3, 114.9, 105.0, 101.1, 97.0, 94.5, 92.5, 68.4, 68.1, 31.4, 31.3, 29.5, 29.2, 28.6, 28.5, 25.6, 25.2, 22.5, 22.2,

13.9, 13.8. ESI-MS: m/z calcd for $([M]^+)$ $C_{105}H_{125}N_5O_8Zn$: 1650.5537; found 1650.5538. mp: 218°C.

2.4 Device fabrication

A compact layer of TiO_2 was deposited on the FTO-coated glass by spray pyrolysis deposition with di-isopropoxytitanium bis(acetyl acetonate) solution. Subsequently a 8 μ m mesoporous TiO_2 (particle size, 20 nm, PASOL HPW-18NR TiO_2 nanopowders, JGC Catalysts and Chemicals Ltd., Japan) transparent electrodes and a 5 μ m scattering layer were prepared by screen printing onto FTO-coated conducting glass layer by layer, which were sintered at 500°C for 30min, respectively. Then The working electrode was prepared by immersing TiO_2 film into the 0.2mM dye solution (in Toluene/EtOH = 1/1, v/v) containing chenodeoxycholic acid (CDCA, 0.4 mM) at 25°C overnight. A thermally platinized FTO glass counter electrode and the working electrode were then sealed with a 25 μ m thick hot-melt film (Surlyn, Dupont) by heating the system at 100 °C. After sealing, the liquid electrolyte was injected into the cell through the hole predrilled in counter electrode and then the hole was sealed with Surlyn polymer and cover glass. The liquid electrolyte (Z959) consisted of 1.0 M 1,3-dimethylimidazolium iodide (DMII), 0.03M iodine, 0.1M guanidinium thiocyanate and 0.5M tert-butylpyridine in a mixture of acetonitrile/valeronitrile (85: 15, v/v).

2.5 Photovoltaic measurements

The complete DSSCs prepared under the same conditions were used to measure I-V, IPCE and EIS. Current-voltage ($I-V$) characteristics were measured with a

Keithley 2400 source/meter and a Newport solar simulator (model 91160) giving light with AM 1.5 G spectral distribution, which was calibrated using a certified reference solar cell (Fraunhofer ISE) to an intensity 100 mW cm^{-2} . A black mask with a slightly smaller circular aperture (0.159 cm^2) than the active area of the square solar cell (0.25 cm^2) was applied on top of the cell. The incident photon-to-current conversion efficiency (IPCE) was measured using a 150W xenon lamp (Oriel) fitted with a monochromator (Cornerstone 260) as monochromatic light source. The illumination spot size was chosen to be slightly smaller than the active area of the DSSC test cells. IPCE photocurrents were recorded under short-circuit conditions using a Keithley 2400 source meter. The monochromatic photon flux was quantified by means of a calibrated silicon photodiode. Electrochemical impedance spectroscopy (EIS) of the symmetric cell was measured using PARSTAT 2273 Electrochemical Workstation in the frequency range 0.1 to 10^6 Hz with 10 mV AC amplitude. The electrolyte used was the same as that used for the fully functional DSSCs. The distance between two electrodes was $45 \mu\text{m}$ and the active area was 0.8 cm^2 .

3. Results and discussion

3.1 Synthesis

In the present work, three porphyrin dyes with different alkyl chains at donor were designed and synthesized for DSSCs based on I^-/I_3^- electrolyte. Thereinto, **YD20** dye reported previously³² is utilized as reference dye to better understand the influence of different alkyl chains at donors on the photovoltaic parameters of DSSCs. The structures of dyes are shown in Fig. 1 and the synthetic scheme and detailed

synthetic procedures are presented in Scheme 1 and experimental section, respectively.

The molecular structures of all target porphyrins and intermediates were confirmed by

^1H NMR, ^{13}C NMR and APCI/ESI-MS, which are given in experimental section.

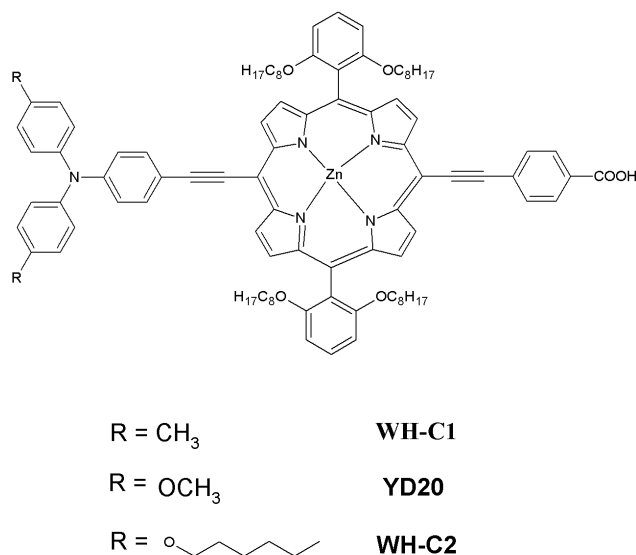
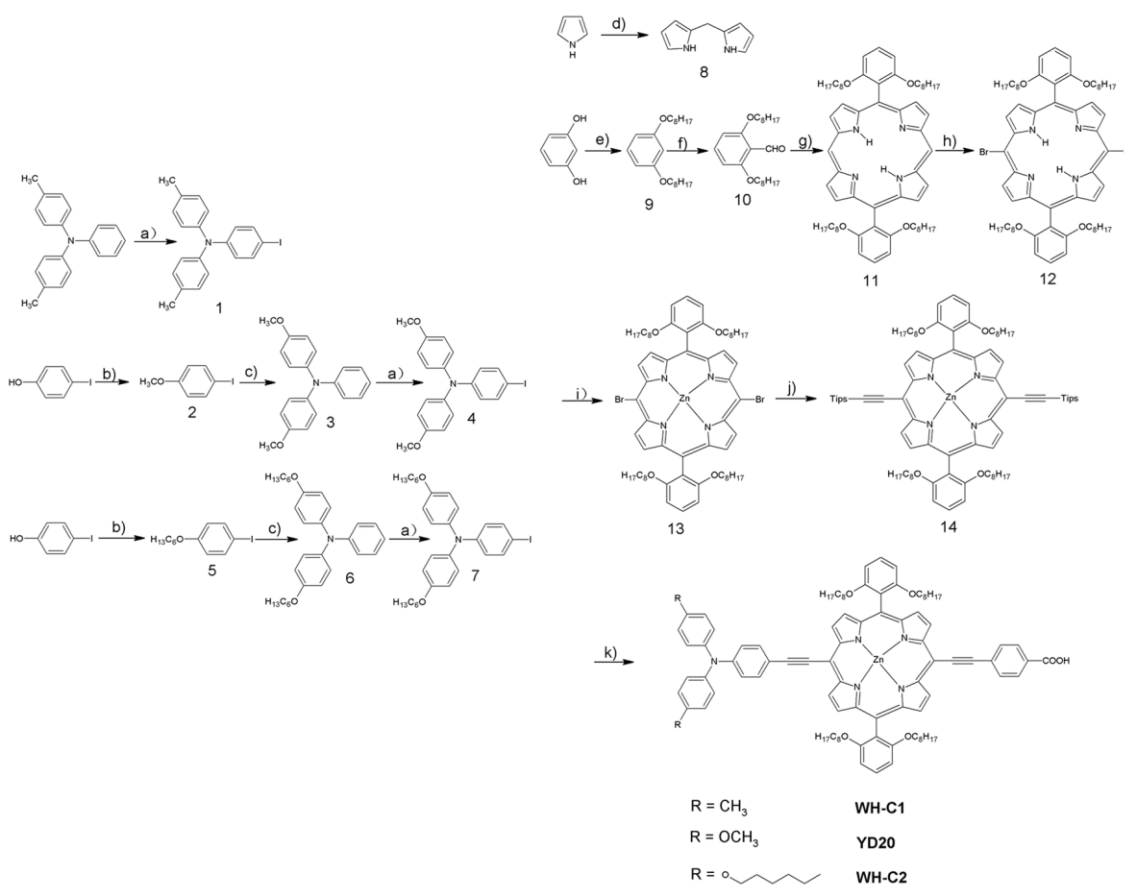


Fig. 1 Molecular structures of sensitizers in this study.



Scheme 1. Synthetic routes of dyes **WH-C1**, **YD20** and **WH-C2**. Reaction conditions:

a) KI, KIO₃, CH₃COOH, 118 °C; b) 1-bromohexane/CH₃I, K₂CO₃, acetone, 60 °C, overnight; c) aniline, 1,10-Phenanthroline, CuCl, KOH, toluene, overnight; d) HCHO, CF₃COOH, RT, 15 min; e) 1-bromooctane, K₂CO₃, acetone, 60 °C, 4 d; f) (i) n-butyl-lithium, TMEDA, THF, 0 °C, 3 h; (ii) DMF, RT, 2 h; g) (i) **8**, CF₃COOH, CH₂Cl₂, RT, 4 h; (ii) DDQ, 1 h; h) NBS, pyridine, CHCl₃, 0 °C, 0.5 h; i) Zn(OAc)₂ 2H₂O, Methanol/CH₂Cl₂, RT, 3 h; j) (triisopropylsilyl)acetylene, Pd(PPh₃)₂Cl₂, CuI, Triethylamine, THF, 65 °C, 6 h; k) (i) TBAF in THF, THF, RT, 0.5 h; (ii) **1/4/7**, 4-iodobenzoic acid, Pd₂(dba)₃, AsPh₃, triethylamine, THF, 65 °C, 5-8 h.

3.2 Optical properties

The UV-vis absorption spectra of **WH-C1**, **YD20** and **WH-C2** in THF solution are depicted in Fig. 2(a). The corresponding peak positions and molar absorption coefficients (ϵ) of Soret and Q bands were listed in Table 1. As shown in Fig. 2, the three sensitizers exhibit typical porphyrin absorption characteristics with a strong Soret band appearing in the range of 400-500nm and mild Q bands appearing in the longer wavelength range of 600-700nm, which is attributed to π - π^* charge transfer transitions of the conjugated molecule and intramolecular charge transfer (ICT) transitions of the D- π -A conjugated backbone.¹⁷ From the absorption data in Table 1, it is shown that Soret band and Q band peak positions for **WH-C2**, **YD20** and **WH-C1** are nearly same. However, on one hand, Soret band and Q band of **WH-C2** and **YD20** are broadened and red-shifted upon introduction of alkoxy chains to donor at the meso-position opposite to the anchoring benzoic acid group.⁴⁸ On the other hand, the measured peak molar extinction coefficients (ϵ) of Soret band and Q band for three different porphyrin dyes show significant difference. Compared with **WH-C1**, both **WH-C2** and **YD20** with alkoxy exhibit stronger absorption at Soret band and Q band, which may be ascribed to stronger electron-donating ability of hexyloxy and methoxy.⁴⁸ It is clear that the molar extinction coefficients of three dyes normally increase with increasing alkyl chain length, in agreement with the literature reported previously.³⁵ The enhanced molar extinction coefficient may favor light harvesting and improve monochromatic incident photon-to-current conversion efficiency (IPCE) for DSSCs based on these sensitizers. Meanwhile, Fig. 2(b)

presents the UV-visible absorption spectra of the sensitizers adsorbed on TiO₂ films. In comparison with absorption spectra in solution, the trend of the Soret and Q bands absorption spectra is similar when the sensitizers are adsorbed on TiO₂ films. Nevertheless, the Soret and Q absorption bands are broadened and red-shifted conspicuously. This phenomenon is believed to result from the formation of J-aggregates.^{13, 49, 50} Additionally, the fluorescent emission spectra were measured in THF and shown in Fig. 3. For the fluorescence spectra, major emission bands are observed at 677, 677 and 679 nm for **WH-C2**, **YD20** and **WH-C1**, respectively, which are similar to the trend of the Soret band absorption spectra. Therefore, it can be concluded that the light-capturing ability of the high molar extinction coefficient Zn porphyrin dyes can be enhanced by rational design of the electron donating moieties.^{47, 51}

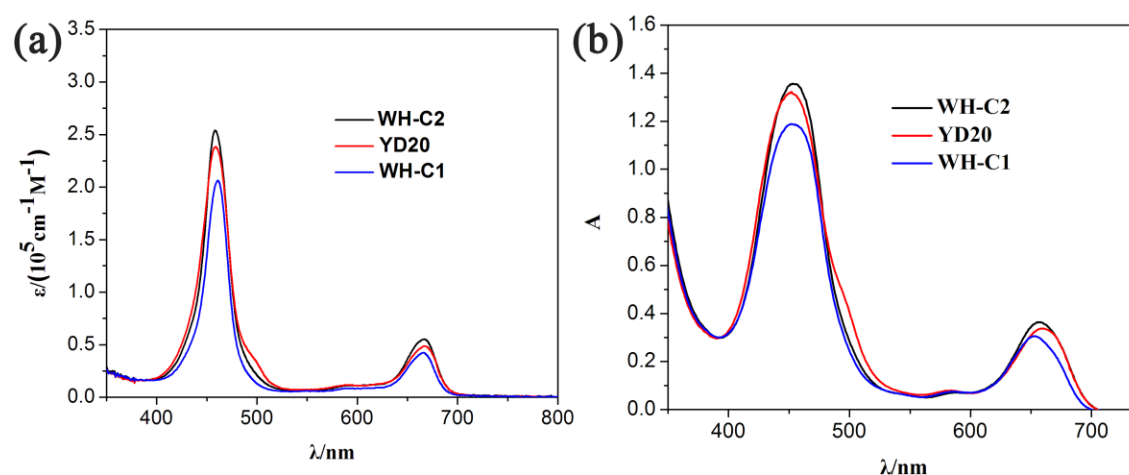


Fig. 2 UV-visible absorption spectra of sensitizers. (a) in THF solvent; (b) adsorbed on TiO₂ films.

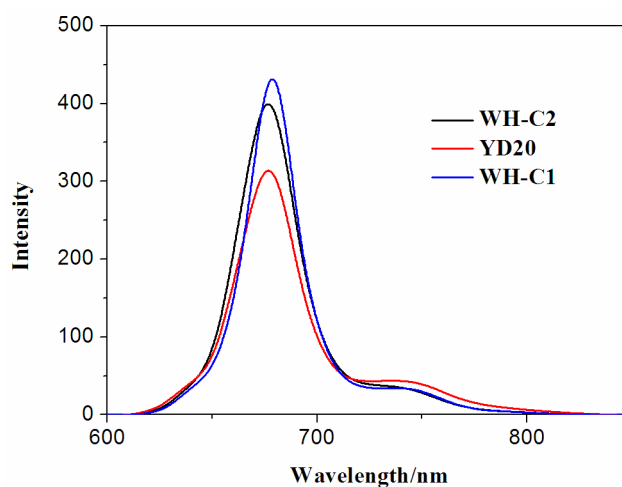


Fig. 3 Emission spectra of sensitizers in THF solvent.

Table 1 Photophysical and electrochemical properties of the sensitizers.

Dye	λ_{\max}^a /nm ($\epsilon/10^4\text{M}^{-1}\text{cm}^{-1}$)	Emission ^a λ_{\max} /nm	E_{ox}^b /V(vs. NHE)	E_{0-0}^c /V(vs. NHE)	E_{LUMO}^d /V(vs. NHE)	Dye loading ^e / 10^{-7} mol cm^{-2}
WH-C2	458(25.39),667(5.53)	677	0.82	1.989	-1.169	0.36
YD20	459(23.83),667(4.87)	677	0.81	1.998	-1.188	0.35
WH-C1	461(20.61),666(4.24)	679	0.86	1.976	-1.116	0.35

^a Absorption and emission data were measured in THF at 25 °C. Excitation wavelengths: 458 nm (**WH-C2**), 459 nm (**YD20**), 461nm (**WH-C1**). ^b The first porphyrin-ring oxidation was performed at 25 °C with each porphyrin (0.5 mM) in THF containing TBAPF₆(0.1M) under N₂ condition with a GC working electrode, a Pt counter electrode, and a Ag/AgCl reference electrode with a scan rate of 50 mV s⁻¹. ^c E_{0-0} was estimated from the intersection wavelengths of the normalized UV/Vis absorption and fluorescence spectra. ^d $E_{\text{LUMO}} = E_{\text{ox}} - E_{0-0}$. ^e the amount of porphyrin

dyes were carried out through the desorption of a 5 μm thick TiO_2 film sensitized by dye in the 0.05 M solution of NaOH in THF/EtOH/ H_2O (v/v/v, 1:1:1) for 2 days.

3.3 Electrochemical properties

In order to investigate the feasibility of electron injection and dye regeneration processes in DSSCs, Cyclic voltammetry measurements for the three dyes were performed in water-free THF containing 0.1 M tetrabutylammonium hexafluorophosphate (TBAPF_6) as the supporting electrolyte and cyclic voltammograms are displayed in Fig. 4. It is observed that electrochemical data for three dyes display quasi-reversible couples. The highest-occupied molecular orbitals (HOMOs) of dyes corresponding to the first redox potential were calculated to be 0.82, 0.81 and 0.86V for **WH-C2**, **YD20** and **WH-C1**, respectively. Practically, it was confirmed that η_{inj} with unit efficiency requires approximately 0.2 V of over-potential ($-\Delta G$) between the TiO_2 conduction band (CB) and lowest unoccupied molecular orbital (LUMO) level of dye, and 0.3 V of $-\Delta G$ between the dye highest occupied molecular orbital (HOMO) level and redox potential for sufficient driving forces of electron injection from the dye to the CB of TiO_2 and the regeneration of oxidized dye.^{5, 52} It is observed that the HOMO levels of three porphyrin dyes are sufficiently more positive than the iodine/iodide redox potential value (0.4 V vs. NHE),⁵³ guaranteeing the efficient regeneration of oxidized dye through I^- presented in the electrolyte of the DSSCs. The zero-zero excitation energies (E_{0-0}) were calculated to be 1.989 V (**WH-C2**), 1.998 V (**YD20**) and 1.976 V (**WH-C1**) by the intersection of the normalized UV-vis absorption spectrum and steady-state fluorescence emission

spectrum. The lowest-unoccupied molecular orbitals (LUMOs) levels of all porphyrin sensitizers were determined according to the expression of $LUMO = HOMO - E_{0-0}$ and corresponding level values are summarized in Table 1. Obviously, the LUMO levels of all dyes are sufficiently more negative compared with the conduction band edge level (E_{cb}) of the TiO_2 electrode (-0.5 V vs. NHE), which means that electron injection from the excited dye into the conduction band of TiO_2 is thermodynamically feasible. Therefore, the three dyes are properly used as sensitizers for DSSCs.

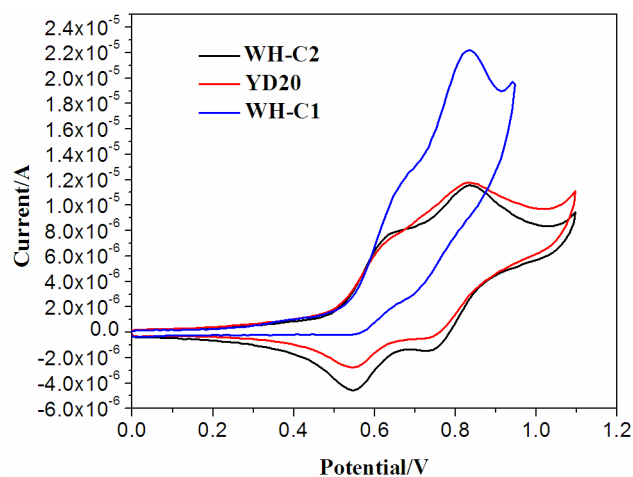


Fig. 4 Cyclic voltammograms of sensitizers in THF at a scan rate of 50 mV/s at room temperature with 0.1 M tetra-n-butylammonium hexafluorophosphate ($TBAPF_6$) as the supporting electrolyte. GC working electrode, Pt wire counter electrode, and Ag/AgCl reference electrode were used.

3.4 Photovoltaic performance of DSSCs

Monochromatic incident photon-to-current conversion efficiency (IPCE) for DSSCs is expressed as follows:^{5, 54}

$$IPCE(\lambda) = \eta_{LHE} \eta_{inj} \eta_{cc}$$

where η_{LHE} is the light harvesting efficiency, η_{inj} is the electron injection yield from

the photo-excited dye into TiO_2 , and η_{cc} is the charge collection efficiency at the electrodes. Among them, η_{LHE} contributes to improvement of IPCE greatly. The IPCEs for DSSCs based on the three dyes are presented in Fig. 5. As shown in Fig. 5, it is observed obviously that two peaks are located in the range of 400-500nm and 600-700nm, respectively, which is consistent with UV-visible absorption spectra of the three dyes. As presented in Fig. 2(a), the molar extinction coefficients at Soret and Q bands for the three dyes are in order of **WH-C2** > **YD20** > **WH-C1**. It is found easily that the IPCEs for DSSCs based on the three dyes have same order with above. Compared with **WH-C1**, higher IPCEs of **WH-C2** and **YD20** are put down to their higher molar extinction coefficients and light harvesting efficiency. Additionally, IPCEs for **WH-C2**, **YD20** and **WH-C1** cover the whole UV-Visible absorption range with the maxima of 66% at 460 nm, 63% at 460 nm and 55% at 450 nm, respectively. It is shown that the maximum IPCE of **WH-C2** dye was increased by 4.5% compared to that of reference dye **YD20**. Consequently, it is demonstrated that introduction of long alkoxy chain can enhance the molar extinction coefficients at Soret and Q bands for porphyrins and result in an improvement of IPCEs.^{35,48}

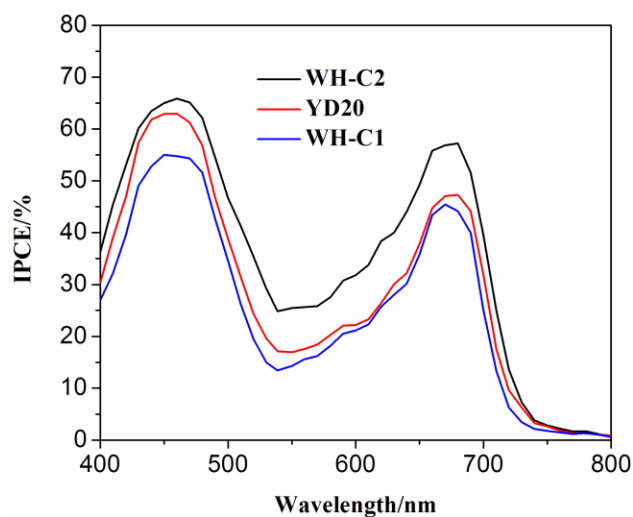


Fig. 5 Action spectra of monochromatic incident photon-to-current conversion efficiency (IPCE) for DSSCs based on **WH-C1**, **YD20** and **WH-C2**. Black: **WH-C2**, red: **YD20**, and blue: **WH-C1**.

The current density-voltage (I-V) characteristic of the DSSCs sensitized by **WH-C2**, **YD20** and **WH-C1** is displayed in Fig. 6 and Table 2. Under standard global air mass 1.5 solar conditions, the **WH-C1** sensitized cell gave a short circuit photocurrent density (J_{sc}) of 11.87 mA cm⁻², an open circuit voltage (V_{oc}) of 814.06 mV, and a fill factor (FF) of 0.69, corresponding to an overall conversion efficiency (η) of 6.71%. Under the same conditions, the DSSCs for **WH-C2** and **YD20** with incorporation of hexyloxy or methoxy groups on the triphenylamine donor segment showed J_{sc} of 13.10 and 12.54 mA cm⁻², V_{oc} of 831.10 and 817.71 mV, and FF of 0.70 and 0.68, corresponding to η of 7.77% and 7.02%, respectively. To account for the influence of the substituent groups of the dyes on the J_{sc} value, the amount of dyes adsorbed on the TiO₂ film was measured. It could be found in Table 1 that the adsorbed amounts of 0.36×10^{-7} mol cm⁻² for **WH-C2**, 0.35×10^{-7} mol cm⁻² for **YD20**, and 0.35×10^{-7} mol cm⁻² for **WH-C1** are almost the same. Therefore, it is obvious that the enhanced J_{sc} is not originated from their adsorbed amounts. Apparently, J_{sc} of DSSCs based on the three sensitizers increases with the elongation of alkyl chains in the order of **WH-C1** < **YD20** < **WH-C2**, which is in accordance with the electron-donating ability of alkyl chains namely methyl < methoxy < hexyloxy. Actually, the order of J_{sc} of DSSCs with the three sensitizers is in good agreement with the trend of molar extinction coefficients (as shown in Fig. 2) and IPCEs. In comparison with **WH-C1** and **YD20**, J_{sc} of **WH-C2**-sensitized solar cell is enhanced by 10.4% and 4.5%, respectively. So it has been well documented that the incorporation of the long alkoxy chain at donor is beneficial to intramolecular charge transfer and improve the short circuit current dramatically. The photocurrents integrated from the IPCE spectra of **WH-C2**, **YD20** and **WH-C1** give a current density of 11.83, 10.79 and 10.16 mA cm⁻², respectively, which is in good agreement

with the measured photocurrent density. In addition, as seen from Table 2 and Fig. 6, the V_{oc} of the devices sensitized by the three porphyrin dyes follows the order: $V_{oc}(\mathbf{WH-C2}) > V_{oc}(\mathbf{YD20}) > V_{oc}(\mathbf{WH-C1})$. It is clear that the V_{oc} of DSSCs with **YD20** is only higher about 4 mV than that of DSSCs with **WH-C1**, which might be ascribed to their same alkyl chain length. Compared with **YD20**, **WH-C2**-sensitized solar cell exhibits an open circuit voltage increase of 13.39 mV. The result is explained through long hexyl chain that can prevent charge recombination between the electron injected into the conduction band of TiO_2 and I_3^- at the vicinity of TiO_2 .^{27, 39, 40, 48, 55}

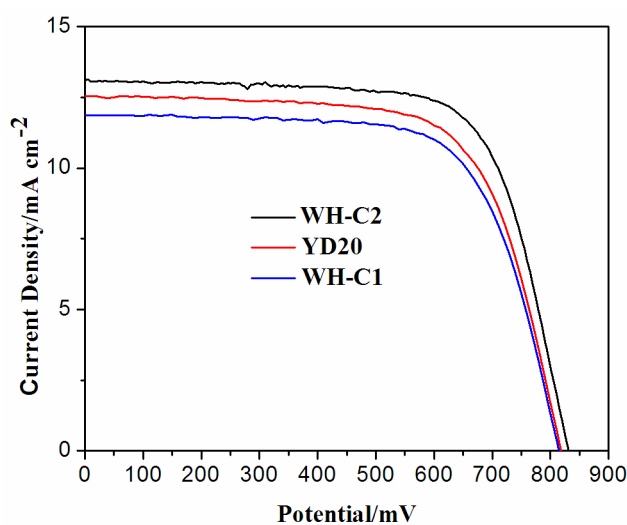


Fig. 6 Current-voltage characteristics of DSSCs sensitized with **WH-C1**, **YD20** and **WH-C2** under AM 1.5 G simulated solar light (100 mW cm^{-2}). Black: **WH-C2**, red: **YD20**, and blue: **WH-C1**.

Table 2 The photovoltaic performance parameters^a of the DSSCs employing **WH-C1**, **YD20** and **WH-C2** under AM 1.5 G simulated solar light (100 mW cm^{-2}).

Dye	V_{oc}/mV	$J_{sc}/\text{mA cm}^{-2}$	FF	$\eta/\%$	R_{rec}/Ω	τ_e/ms
WH-C2	831.09 ± 4	13.10 ± 0.24	0.70 ± 0.014	7.77 ± 0.12	365.2	33.99
YD20	817.71 ± 2	12.54 ± 0.20	0.68 ± 0.006	7.02 ± 0.06	121.6	24.80
WH-C1	814.06 ± 3	11.87 ± 0.28	0.69 ± 0.008	6.71 ± 0.05	72.0	19.86

^a The photovoltaic parameters are averaged values obtained from analysis of the J - V

curves of three identical devices fabricated and characterized under the same experimental conditions for each dye. The uncertainties represent two standard deviations of the measurements.

3.5 Electrochemical impedance spectroscopy (EIS)

To further investigate and elucidate the photovoltaic results and obtain more interfacial charge transfer information of the DSSC with the different dyes, electrochemical impedance spectroscopy (EIS) was also performed in the dark under a forward bias of -0.6V. The Nyquist and Bode plots for **WH-C2**, **YD20** and **WH-C1** are shown in Fig. 7. As shown in the Nyquist plots (Fig. 7(a)), in the high frequency range over 10^6 Hz, the impedance is dominated by the ohmic serial resistance (R_s) of the dummy cell owing to the square resistance of FTO glass substrate, where the phase is zero.^{5,56} As seen in Fig. 7(a), the first semicircle is assigned to impedances related to charge transport at the electrolyte/counter electrode interface. In the middle frequency range, the large semicircle is ascribed to the electron recombination resistance (R_{rec}) and chemical capacitance at the working electrode /electrolyte.^{57,58} It is obvious that the semicircle resulting from R_{rec} based on different dyes is in the order of **WH-C1** < **YD20** < **WH-C2**, indicating that the electron recombination resistance augments from **WH-C1** to **WH-C2**.⁵ Considering that the different length of the alkyl chains, it could be concluded that the longer alkyl chain usually produce a higher recombination resistance. It is well known that the photovoltage of a DSSC is intrinsically influenced by the degree of electron recombination reaction.⁵⁹ Based on the above conclusions, the order of the V_{oc} (**WH-C1** < **YD20** < **WH-C2**) could be

attributed to different electron recombination resistances caused by different alkyl chains. In the Bode phase plots Fig. 7(b), the middle-frequency peak stands for the charge-transfer process of injected electrons in TiO_2 corresponding to the second semicircle in Nyquist plots. The Bode phase plots likewise demonstrate the differences in the R_{rec} . Electron lifetime calculated through the relation $\tau_e = 1/(2\pi f)$ (f is the peak frequency of middle-frequency range in EIS Bode plot)⁶⁰ can well explain the higher V_{oc} of **WH-C2**-sensitized solar cells compared with that of **WH-C1** and **YD20**. Electron lifetime τ_e was determined to be 19.86, 24.80 and 33.99 ms, for **WH-C1**, **YD20** and **WH-C2**, respectively. The higher electron lifetime τ_e observed from **WH-C2** indicated more effective repression of the charge recombination back reaction, which could be reflected in the improvements of V_{oc} , resulting in improved device efficiency. In a word, it has been demonstrated that incorporation of long alkoxy chain not only can enhance molar extinction coefficients of dyes but can also act as blocking layer through suppression of recombination reaction between the electron injected into the conduction band of TiO_2 and I_3^- at the vicinity of TiO_2 .

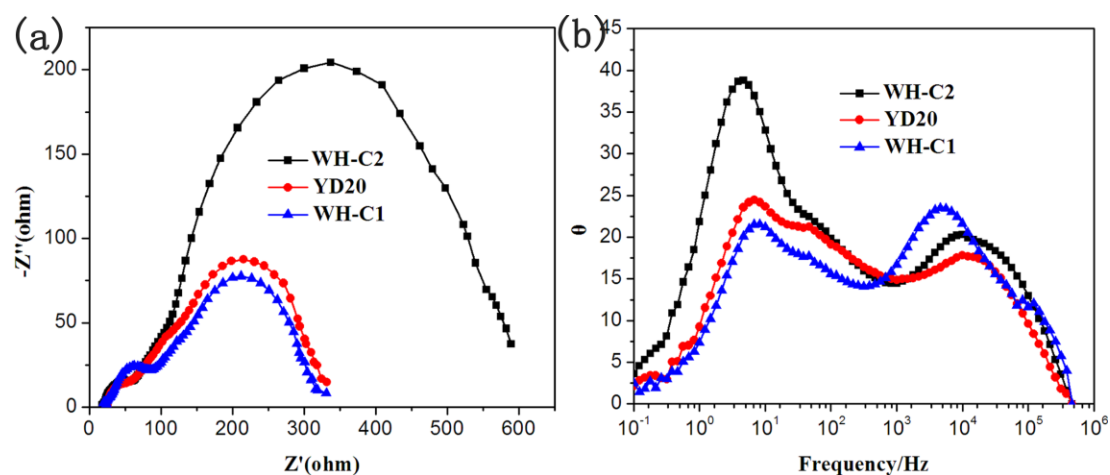


Fig. 7 Electrochemical impedance spectroscopy (EIS) for DSSCs based on the

sensitizers. (a) Nyquist plots; (b) Bode phase plots in the dark under a forward bias of -0.6 V.

4. Conclusions

In summary, we designed and synthesized a series of novel push-pull porphyrins possessing different alkyl chain substituents with electron-donating ability at donors. In order to systematically investigate the effect of different electron-donating ability alkyl chains substituents at donors on the photovoltaic performance of the porphyrin-sensitized solar cells, we performed UV-vis absorption, cyclic voltammetry, photovoltaic performance, electrochemical impedance spectroscopy measurements and so on. The V_{oc} and J_{sc} of the devices sensitized by the three porphyrin dyes follows the order: **WH-C2** > **YD20** > **WH-C1**. Under standard global air mass 1.5 solar conditions, the highest power conversion efficiency was achieved by the solar cell based on **WH-C2** sensitizer with a long alkoxy group, which gave a short circuit photocurrent density (J_{sc}) of 13.10 mA cm⁻², an open circuit voltage (V_{oc}) of 831.09 mV, and a fill factor (ff) of 0.70, corresponding to an overall conversion efficiency (η) of 7.77%. This study demonstrates that incorporation of long alkoxy chain is an effective method to enhance the molar extinction coefficients of dyes, suppress dye aggregation and recombination. For the purpose of further improving the power conversion efficiency of porphyrin-sensitized solar cells, further elaborate and rational design is of the essence.

Acknowledgements

The authors acknowledge the financial support by the Ministry of Science and Technology of China (863, No. SS2013AA50303), the National Natural Science Foundation of China (Grant No. 61106056), the fundamental Research Funds for the Central Universities (HUSTNY022), and Scientific Research Foundation for Returned Scholars, Ministry of Education of China. We also thank the Analytical and Testing Center of Huazhong University of Science and Technology [HUST] for NMR, MS, UV-vis absorption and emission spectra measurements.

References

- 1 B. O'Regan and M. Gratzel, *Nature*, 1991, **353**, 737.
- 2 A. Hagfeldt, G. Boschloo, L. Sun, L. Kloo and H. Pettersson, *Chem. Rev.*, 2010, **110**, 6595.
- 3 B. E. Hardin, H. J. Snaith and M. D. McGehee, *Nat. Photonics*, 2012, **6**, 162.
- 4 C. Grätzel and S. M. Zakeeruddin, *Mater. Today*, 2013, **16**, 11.
- 5 S. Zhang, X. Yang, Y. Numata and L. Han, *Energ. Environ. Sci.*, 2013, **6**, 1443.
- 6 M. K. Nazeeruddin, F. De Angelis, S. Fantacci, A. Selloni, G. Viscardi, P. Liska, S. Ito, B. Takeru and M. Grätzel, *J. Am. Chem. Soc.*, 2005, **127**, 16835.
- 7 Y. Chiba, A. Islam, Y. Watanabe, R. Komiya, N. Koide and L. Han, *Japanese Journal of Applied Physics*, 2006, **45**, L638.
- 8 F. Gao, Y. Wang, D. Shi, J. Zhang, M. Wang, X. Jing, R. Humphry-Baker, P. Wang, S. M. Zakeeruddin and M. Grätzel, *J. Am. Chem. Soc.*, 2008, **130**, 10720.
- 9 L. Han, A. Islam, H. Chen, C. Malapaka, B. Chiranjeevi, S. Zhang, X. Yang and M. Yanagida, *Energ. Environ. Sci.*, 2012, **5**, 6057.

- 10 B. G Kim, K. Chung and J. Kim, *Chem. Eur. J.*, 2013, **19**, 5220.
- 11 C. W. Lee, H. P. Lu, C. M. Lan, Y. L. Huang, Y. R. Liang, W. N. Yen, Y. C. Liu, Y. S. Lin, E. W. G Diau and C. Y. Yeh, *Chem. Eur. J.*, 2009, **15**, 1403.
- 12 W. Zhou, B. Zhao, P. Shen, S. Jiang, H. Huang, L. Deng and S. Tan, *Dyes Pigments*, 2011, **91**, 404.
- 13 C.-Y. Lin, C.-F. Lo, L. Luo, H.-P. Lu, C.-S. Hung and E. W.-G Diau, *J. Phys. Chem. C*, 2008, **113**, 755.
- 14 J. K. Park, J. Chen, H. R. Lee, S. W. Park, H. Shinokubo, A. Osuka and D. Kim, *J. Phys. Chem. C*, 2009, **113**, 21956.
- 15 M. V. Martínez-Díaz, G de la Torre and T. Torres, *Chem. Commun.*, 2010, **46**, 7090.
- 16 L.-L. Li and E. W.-G Diau, *Chem. Soc. Rev.*, 2013, **42**, 291.
- 17 H. Imahori, T. Umeyama and S. Ito, *Acc. Chem. Res.*, 2009, **42**, 1809.
- 18 T. Higashino and H. Imahori, *Dalton Transactions*, 2015, **44**, 448.
- 19 M. Urbani, M. Grätzel, M. K. Nazeeruddin and T. s. Torres, *Chem. Rev.*, 2014, **114**, 12330..
- 20 H.-P. Lu, C.-L. Mai, C.-Y. Tsia, S.-J. Hsu, C.-P. Hsieh, C.-L. Chiu, C.-Y. Yeh and E. W.-G Diau, *Phys. Chem. Chem. Phys.*, 2009, **11**, 10270.
- 21 C.-P. Hsieh, H.-P. Lu, C.-L. Chiu, C.-W. Lee, S.-H. Chuang, C.-L. Mai, W.-N. Yen, S.-J. Hsu, E. W.-G Diau and C.-Y. Yeh, *J. Mater. Chem.*, 2010, **20**, 1127.
- 22 T. Bessho, S. M. Zakeeruddin, C. Y. Yeh, E. W. G Diau and M. Grätzel, *Angew. Chem. Int. Ed.*, 2010, **49**, 6646.

- 23 S.-L. Wu, H.-P. Lu, H.-T. Yu, S.-H. Chuang, C.-L. Chiu, C.-W. Lee, E. W.-G. Diau and C.-Y. Yeh, *Energ. Environ. Sci.*, 2010, **3**, 949.
- 24 M. J. Lee, K. D. Seo, H. M. Song, M. S. Kang, Y. K. Eom, H. S. Kang and H. K. Kim, *Tetrahedron Lett.*, 2011, **52**, 3879.
- 25 C.-L. Wang, Y.-C. Chang, C.-M. Lan, C.-F. Lo, E. W.-G. Diau and C.-Y. Lin, *Energ. Environ. Sci.*, 2011, **4**, 1788.
- 26 Y.-C. Chang, C.-L. Wang, T.-Y. Pan, S.-H. Hong, C.-M. Lan, H.-H. Kuo, C.-F. Lo, H.-Y. Hsu, C.-Y. Lin and E. W.-G. Diau, *Chem. Commun.*, 2011, **47**, 8910.
- 27 N. Koumura, Z.-S. Wang, S. Mori, M. Miyashita, E. Suzuki and K. Hara, *J. Am. Chem. Soc.*, 2006, **128**, 14256.
- 28 K. Kurotobi, Y. Toude, K. Kawamoto, Y. Fujimori, S. Ito, P. Chabera, V. Sundström and H. Imahori, *Chem. Eur. J.*, 2013, **19**, 17075.
- 29 Y. Wang, B. Chen, W. Wu, X. Li, W. Zhu, H. Tian and Y. Xie, *Angew. Chem. Int. Ed.*, 2014, **53**, 10779.
- 30 J. Luo, M. Xu, R. Li, K.-W. Huang, C. Jiang, Q. Qi, W. Zeng, J. Zhang, C. Chi and P. Wang, *J. Am. Chem. Soc.*, 2013, **136**, 265.
- 31 A. Yella, H.-W. Lee, H. N. Tsao, C. Yi, A. K. Chandiran, M. K. Nazeeruddin, E. W.-G. Diau, C.-Y. Yeh, S. M. Zakeeruddin and M. Grätzel, *Science*, 2011, **334**, 629.
- 32 T. Ripolles-Sanchis, B.-C. Guo, H.-P. Wu, T.-Y. Pan, H.-W. Lee, S. R. Raga, F. Fabregat-Santiago, J. Bisquert, C.-Y. Yeh and E. W.-G. Diau, *Chem. Commun.*, 2012, **48**, 4368.

- 33 S. Mathew, A. Yella, P. Gao, R. Humphry-Baker, B. F. Curchod, N. Ashari-Astani, I. Tavernelli, U. Rothlisberger, M. K. Nazeeruddin and M. Grätzel, *Nat. Chem.*, 2014, **6**, 242.
- 34 T. M. Viseu, G. Hungerford and M. I. C. Ferreira, *J. Phys. Chem. B*, 2002, **106**, 1853.
- 35 Q.-Y. Yu, J.-Y. Liao, S.-M. Zhou, Y. Shen, J.-M. Liu, D.-B. Kuang and C.-Y. Su, *J. Phys. Chem. C*, 2011, **115**, 22002.
- 36 N. Cai, S.-J. Moon, L. Cevey-Ha, T. Moehl, R. Humphry-Baker, P. Wang, S. M. Zakeeruddin and M. Grätzel, *Nano Lett.*, 2011, **11**, 1452.
- 37 H. N. Tsao, C. Yi, T. Moehl, J. H. Yum, S. M. Zakeeruddin, M. K. Nazeeruddin and M. Grätzel, *ChemSusChem*, 2011, **4**, 591.
- 38 L. Schmidt-Mende, J. E. Kroeze, J. R. Durrant, M. K. Nazeeruddin and M. Grätzel, *Nano Lett.*, 2005, **5**, 1315.
- 39 J. E. Kroeze, N. Hirata, S. Koops, M. K. Nazeeruddin, L. Schmidt-Mende, M. Grätzel and J. R. Durrant, *J. Am. Chem. Soc.*, 2006, **128**, 16376.
- 40 S.-J. Moon, J.-H. Yum, R. Humphry-Baker, K. M. Karlsson, D. P. Hagberg, T. Marinado, A. Hagfeldt, L. Sun, M. Grätzel and M. K. Nazeeruddin, *J. Phys. Chem. C*, 2009, **113**, 16816.
- 41 Y. Cao, Y. Bai, Q. Yu, Y. Cheng, S. Liu, D. Shi, F. Gao and P. Wang, *J. Phys. Chem. C*, 2009, **113**, 6290.
- 42 K. Do, D. Kim, N. Cho, S. Paek, K. Song and J. Ko, *Org. Lett.*, 2011, **14**, 222.
- 43 Y. Wu, H. Guo, T. D. James and J. Zhao, *J. Org. Chem.*, 2011, **76**, 5685.

- 44 L.-L. Tan, L.-J. Xie, Y. Shen, J.-M. Liu, L.-M. Xiao, D.-B. Kuang and C.-Y. Su, *Dyes Pigments*, 2014, **100**, 269.
- 45 R. Li, J. Liu, N. Cai, M. Zhang and P. Wang, *J. Phys. Chem. B*, 2010, **114**, 4461.
- 46 M. Balaz, H. A. Collins, E. Dahlstedt and H. L. Anderson, *Org. Biomol. Chem.*, 2009, **7**, 874.
- 47 J. Lu, X. Xu, Z. Li, K. Cao, J. Cui, Y. Zhang, Y. Shen, Y. Li, J. Zhu and S. Dai, *Chem. Asian J*, 2013, **8**, 956.
- 48 S. H. Kang, I. T. Choi, M. S. Kang, Y. K. Eom, M. J. Ju, J. Y. Hong, H. S. Kang and H. K. Kim, *J. Mater. Chem. A*, 2013, **1**, 3977.
- 49 K. Hara, M. Kurashige, Y. Dan-oh, C. Kasada, A. Shinpo, S. Suga, K. Sayama and H. Arakawa, *New J. Chem.*, 2003, **27**, 783.
- 50 J.-J. Kim, H. Choi, J.-W. Lee, M.-S. Kang, K. Song, S. O. Kang and J. Ko, *J. Mater. Chem.*, 2008, **18**, 5223.
- 51 J. Luo, M. Xu, R. Li, K.-W. Huang, C. Jiang, Q. Qi, W. Zeng, J. Zhang, C. Chi, P. Wang and J. Wu, *J. Am. Chem. Soc.*, 2013, **136**, 265.
- 52 T. Daeneke, A. J. Mozer, Y. Uemura, S. Makuta, M. Fekete, Y. Tachibana, N. Koumura, U. Bach and L. Spiccia, *J. Am. Chem. Soc.*, 2012, **134**, 16925.
- 53 M. Wang, C. Grätzel, S. M. Zakeeruddin and M. Grätzel, *Energ. Environ. Sci.*, 2012, **5**, 9394.
- 54 M. K. Nazeeruddin, A. Kay, I. Rodicio, R. Humphry-Baker, E. Müller, P. Liska, N. Vlachopoulos and M. Grätzel, *J. Am. Chem. Soc.*, 1993, **115**, 6382.
- 55 Z.-S. Wang, N. Koumura, Y. Cui, M. Takahashi, H. Sekiguchi, A. Mori, T. Kubo, A.

- Furube and K. Hara, *Chem. Mater.*, 2008, **20**, 3993.
- 56 G. Liu, H. Wang, X. Li, Y. Rong, Z. Ku, M. Xu, L. Liu, M. Hu, Y. Yang and P. Xiang, *Electrochimica Acta*, 2012, **69**, 334.
- 57 L. Han, N. Koide, Y. Chiba and T. Mitate, *Appl. Phys. Lett.*, 2004, **84**, 2433.
- 58 M. Itagaki, K. Hoshino, Y. Nakano, I. Shitanda and K. Watanabe, *J. Power Sources*, 2010, **195**, 6905.
- 59 K. Cao, J. Lu, J. Cui, Y. Shen, W. Chen, A. Getachewalemu, Z. Wang, H. Yuan, J. Xu and M. Wang, *J. Mater. Chem. A*, 2014, **2**, 4945.
- 60 Z. Wan, C. Jia, Y. Duan, L. Zhou, Y. Lin and Y. Shi, *J. Mater. Chem.*, 2012, **22**, 25140.